Central European Journal of Energetic Materials, **2014**, *11*(4), 475-489
ISSN 2353-1843

Modelling and Calculation of the Initial Ignition Gas Pressure Flow through a Rigid Porous Medium in a 100 mm Ignition Simulator

Zhenggang XIAO*, Sanjiu YING, Weidong HE, Fuming XU

School of Chemical Engineering, Nanjing University of Science and Technology, Nanjing, 210094, P. R. China
**E-mail: xiaozhg@njust.edu.cn*

Abstract: To acquire a better understanding of the early ignition phenomena in a 100 mm ignition simulator loaded with a packed propellant bed, a theoretical model of the ignition gas flow through the rigid porous medium was developed. Three pressure gauges were installed in the lateral side of the ignition simulator for post ignition measurement of the chamber pressure. The pseudo-propellant loaded into the chamber was similar in size to the standard 13/19 single-base cylindrical propellant. It was composed of a rigid ceramic composite with low thermal conductivity. It was assumed that the pseudo-propellant bed was rigid in contrast to the assumption of an elastic porous medium. The calculated pressure values were well verified by the experimental data at a low loading density of the pseudo-propellant bed of 0.18 g·cm^{-3}. However, there was still error between the experimental and the calculated results in the early pressure peak position closest to the ignition primer when the loading density of the pseudo-propellant bed was increased to 0.73 and 1.06 g·cm^{-3}. This error is attributed to the change in local permeability of the pseudo-propellant bed at high loading densities, which is assumed, for ease of modelling, to be constant in the model. These calculations may enable a better understanding of the physical processes of ignition gas flow in an ignition simulator loaded with a pseudo-propellant bed.

Keywords: ignition, ignition simulator, porous media, propellant, modelling, simulation

1 Introduction

Ignition of the propellant bed in a gun chamber is the most important event occurring during the early interior ballistic cycle. Ignition of the propellant bed

can be interpreted by two mechanisms [1]: one is the direct or uniform ignition, where the propellant charge is ignited primarily by the efflux of the igniter; another is the indirect or flame spreading ignition, where the igniter efflux ignites only a localized region of the charge, and the resultant propellant gasification promotes a convective flow to ignite the remainder of the charge. Historically, many researchers have investigated the ignition and flame spreading process in granular and ball powder propellants [2-8]. The resultant over-pressurization can create large-scale travelling pressure waves that cause propellant grain fracture and projectile impact loads because of the motion and redistribution of the propellant bed, and even catastrophic failures under conditions of high loading densities of the propellant charge [9].

Therefore, a better understanding of the ignition process and pressure distribution in the propellant bed and the gun chamber in the case of charges with propellant of high loading densities, especially in the early stage of the interior ballistic cycle when the chamber pressure is low, would be of great benefit to the design of ignition systems and gun propellant charges.

A number of previous studies investigated the ignition and flame spreading process associated with anomalous behaviour [9-11]. Meanwhile, many laboratory devices and test rigs have been designed to simulate the early ignition process and flame spreading. In particular, for convective ignition, a dual-chamber hollow cylinder ignition simulator, composed of igniter chamber and flow chamber, was designed by Kooker *et al.* [6] to study the ignition and longitudinal flame spreading in a packed bed of granular propellant, especially of LOVA propellant. The igniter chamber, where a small quantity of ball powder was burned, was sealed, by a diaphragm and a multiple nozzle plate, from the flow chamber which contains the sample of granular propellant grains. Thus the ignition wave was composed of gas phase products only, which was intended to create an environment that is more easily modelled. The experimental data from this kind of flame spreading chamber were particularly valuable in validating predictions for gun propellants within the interior ballistic model. The initial results emphasized an important concept: time to ignition is determined by the competition between the flow residence time and the characteristic time for chemical reaction. The propellant composition and flame structure plays an important role in the control of ignition delays.

Although the early pressure-time history in a simulator can be recorded with a special purpose test rig, we also needed to understand flame spreading and pressure distribution in the simulator by modelling and numerical simulation of the early ignition stage. Based on the modelling and simulation results, we could design and rapidly adjust the ignition system for special propellant charges

based on the interaction between the ignition system and the propelling charge.

Nusca *et al*. [12, 13] applied the multi-dimension flow mechanic to simulate the ignition process in small arms and large-calibre guns under traditional and plasma ignition. It provided key insights into the early initiation phase. Song *et al*. [14] established a porous medium, mechanic-dynamic model for the ignition gas flow compression of the charge bed. The charge bed was assumed to be an elastic medium in the modelling. Obviously, the elastic medium assumption is not a real situation during the early stages of ignition of a propellant bed.

Fluid flow in porous media is of interest for many engineering fields, such as enhanced oil recovery, paper and textile coating, composite manufacturing processes and bioengineering [15-17]. Modelling and numerical simulation based on Darcy's Law can be employed to describe the fluid flow through porous media [18].

Almost anything can be considered as porous, depending on the scale of observation. Generally, we considered porous media as heterogeneous systems consisting of a solid matrix with fluid-filled voids [19].

For the ignition of a high loading density propellant bed, if we assume that the propellant is a porous medium in the simulator and the ignition gas generated by the igniter flows through the porous propellant bed, then Darcy's law can be employed to describe the ignition gas flow process in order to establish the ignition gas pressure distribution in the simulator.

Due to the low permeability of a high loading density propellant bed, when it is ignited, the ignition pressure is established and subsequently drops during the flowing process through the low permeability propellant bed. Many investigations have been conducted in order to understand the flow through porous media. However there is little research on the study of the initial ignition pressure during the early stages of ignition in a 100 mm ignition simulator.

Here we have modified the elastic medium assumption to a rigid porous medium assumption for a special test rig and a pseudo-propellant in a 100 mm ignition simulator. A new theoretical model of the ignition gas, based on the mechanical flow through a rigid porous medium, has been developed in order to interpret the early pressure flow distribution along the simulator axis. This aims to acquire a better understanding of ignition system design for high loading density propellant charges.

2 Experimental setup

Figure 1 depicts a cross-sectional view of a steel 100 mm ignition simulator assembly. The inside diameter of the ignition simulator was 100 mm, and the

length was 535 mm. Three pressure gauges (G1, G2 and G3) were installed in the lateral side of the chamber for measurement of the chamber pressure after ignition. The distance between adjacent pressure gauges was 200 mm. The electrical igniter was at the left end of the simulator. During the experiments, the simulator was positioned vertically with the igniter end at the bottom. The pseudo-propellant loaded into the chamber was similar in size to the standard 13/19 single-base cylindrical propellant. It was composed of a rigid ceramic composite with a low thermal conductivity, and could not be ignited. It should be noted that the ceramic composite consisted of SiO_2 and Al_2O_3. The ceramic composite was the same size as standard 13/19 cylindrical propellant. Its thermal conductivity was in the range of 0.3-1.2 W/(m·K), whereas, the thermal conductivity of single-base propellants is around 0.2-0.4 W/(m·K). Although the thermal conductivity of the ceramic composite was larger than real propellants, this assumption was still used in this paper for the convenience of the calculations.

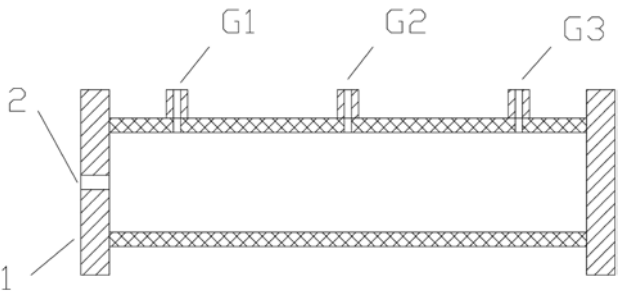

Figure 1. Schematic diagram of the 100 mm ignition simulator (1 − main body; 2 – igniter; G1, G2, G3 are the three pressure gauges).

Table 1. Test conditions for the 100 mm ignition simulator at ambient temperature

Round No.	Loading density [g·cm^{-3}]	Porosity
1	0	0
2	0.18	0.0777
3	0.36	0.1553
4	0.73	0.3107
5	1.06	0.4543

The tests were to determine the pressure rise as a result of ignition of the primer alone in an empty simulator, and the flow characteristics through the pseudo-propellant bed, respectively.

Table 1 lists the test conditions of ignition and the pseudo-propellant bed loaded in the ignition simulator at ambient temperature. The igniter was an electrically ignited, black powder primer. The mass of black powder was 40 g. The volume of the ignition simulator was 5.55 dm^3. The density of the ceramic composite was 2.32 $kg \cdot dm^{-3}$. The maximum porosity in the ignition simulator was 0.45 when it was filled with the ceramic composite pseudo-propellant.

3 Modelling

3.1 Assumptions

Gas phase and solid phase flows were assumed to coexist in the combustion chamber after ignition. The gas phase is composed of igniter combustion gases and air. Although the pseudo-propellant bed cannot be ignited, it can create an environment of a packed bed with low permeability. We assumed that the solid phase did not move during the ignition process. The ignition gas flow in the pseudo-propellant bed depends on the purely "mechanical" process that results from the pressure difference along the simulator, although it also results from the thermal gradient in some cases. The pseudo-propellant was composed of a rigid ceramic composite with low thermal conductivity. It was assumed that it was isotropic. Thus here, we consider the purely "mechanical" process for the purpose of easy modelling, avoiding the complex heat exchange process.

It was assumed that the ignition gas is one-dimensional in the flow through the pseudo-propellant bed in the ignition simulator, and all of the flow parameters are a function of the distance from the igniter end and time.

Since the pseudo-propellant bed is assumed to be rigid, the porosity φ does not change with time and ignition pressure. It is therefore a constant, which can be written as:

$$\frac{\mathrm{d}\varphi}{\mathrm{d}x} = 0 \tag{1}$$

We will not consider the heat exchange process in the ignition simulator. We replaced the energy and gas state equation with the correlation equation between the ignition gas pressure, p, and the density, ρ:

$$p = p_0 \left(\frac{\rho}{\rho_0} \right)^m \tag{2}$$

where m is the multi-exponent, p_0 is the initial pressure, ρ_0 is the gas density at the initial pressure p_0, and ρ is the gas density at pressure p.

3.2 Mathematical equations

For the ignition gas flow through a packed pseudo-propellant bed, Darcy's Law can be used to give the equation:

$$\rho \frac{\mathrm{d}u}{\mathrm{d}t} = -\frac{\partial p}{\partial x} - \frac{L_p \rho (1-\varphi)}{\varphi k_p d_p} u^2 \tag{3}$$

where k_p is the permeability of the packed pseudo-propellant bed, d_p is the average diameter of the packed pseudo-propellant grains, u is the fluid flow velocity in the direction of the pressure gradient, and L_p is the experimental coefficient.

According to the principle of mass conservation, the ignition gas flow through the porous medium can be written as the following continuity equation:

$$\varphi \frac{\partial \rho}{\partial t} + \frac{\partial (\varphi \rho u)}{\partial x} = 0 \tag{4}$$

From the above continuity Equation (4):

$$\varphi \frac{\partial \rho}{\partial t} + \varphi\rho \frac{\partial u}{\partial x} + \varphi u \frac{\partial \rho}{\partial x} + \rho u \frac{\partial \varphi}{\partial x} = 0 \tag{5}$$

According to the basic assumptions and Equation (1):

$$\frac{\partial \varphi}{\partial x} = \frac{\mathrm{d}\varphi}{\mathrm{d}x} = 0 \tag{6}$$

Thus, substituting Equation (6) into Equation (5), there results:

$$\frac{\partial \rho}{\partial t} + u \frac{\partial \rho}{\partial x} + \rho \frac{\partial u}{\partial x} = 0 \tag{7}$$

Equation (7) can be written as:

$$\frac{\mathrm{d}\rho}{\mathrm{d}t} + \rho\frac{\partial u}{\partial x} = 0 \tag{8}$$

From Equation (3):

$$\frac{\partial u}{\partial t} + u\frac{\partial u}{\partial t} + \frac{1}{\rho}\frac{\partial p}{\partial x} = -\frac{L_p\rho(1-\varphi)}{\varphi k_p d_p \rho}u^2 \tag{9}$$

Differentiating Equation (2) we have:

$$\mathrm{d}p = p_0 m\left(\frac{1}{\rho_0}\right)^m \rho^{m-1}\mathrm{d}\rho \tag{10}$$

Equation (10) can be further written as:

$$\frac{\mathrm{d}p}{\mathrm{d}\rho} = \frac{mp}{\rho} \tag{11}$$

From Equation (11) and Equation (8) there results:

$$\frac{\mathrm{d}p}{\mathrm{d}t} + mp\frac{\partial u}{\partial x} = 0 \tag{12}$$

From Equations (7), (9) and (12), we obtained the following basic equations:

$$\begin{cases} \dfrac{\partial\rho}{\partial t} + u\dfrac{\partial\rho}{\partial x} + \rho\dfrac{\partial u}{\partial x} = 0 \\ \dfrac{\partial u}{\partial t} + u\dfrac{\partial u}{\partial x} + \dfrac{1}{\rho}\dfrac{\partial p}{\partial x} = F \\ \dfrac{\partial p}{\partial t} + u\dfrac{\partial p}{\partial x} + mp\dfrac{\partial u}{\partial x} = 0 \end{cases} \tag{13}$$

where

$$F = -\frac{L_p(1-\varphi)}{\varphi k_p d_p \rho}u^2 \tag{14}$$

The basic Equations (13) are hyperbolic equations. The initial conditions are:

$$\begin{cases} u\big|_{t=0} = 0 \\ p\big|_{t=0} = p_0 \end{cases} \tag{15}$$

where p_0 is the initial pressure.

The left boundary conditions of the basic equations are the igniter generated gas flow parameters; the right boundary is the static end wall of the chamber, and can be determined by reflection.

4 Numerical Method

4.1 Differential equation

We used the finite difference method to solve the problem described by Equations (13), subject to the initial and boundary conditions (15).

Two sets of parallel lines:

$$\begin{cases} x = x_j = j\Delta x \quad (j = 0,1,2,\cdots,MM) \\ t = t_n = n\Delta t \quad (n = 1,2,\cdots,NN) \end{cases} \tag{16}$$

were used to divide the cross-section of the 100 mm ignition simulator into a rectangular mesh. In Equation (16), Δt and Δx are the time intervals and distance intervals, respectively.

The basic Equations (13) were solved using the Richtmyer two-step difference method, the subscript letter j denoting the specific position and superscript letter n denoting the time interval. Thus:

$$\begin{cases} U_j^{n+\frac{1}{2}} = \dfrac{1}{2}(U_{j+1}^n + U_{j-1}^n) - \dfrac{\Delta t}{4\Delta x} A_j^n (U_{j+1}^n - U_{j-1}^n) + H_j^n \dfrac{\Delta t}{2} \\ U_j^{n+1} = U_j^n - \dfrac{\Delta t}{2\Delta x} A_j^{n+\frac{1}{2}} (U_{j+1}^{n+\frac{1}{2}} - U_{j-1}^{n+\frac{1}{2}}) + H_j^{n+\frac{1}{2}} \Delta t \end{cases} \tag{17}$$

4.2 Numerical stability

The stability conditions for the Richtmyer two-step difference method are the Courant conditions for the explicit numerical calculation of typical hyperbolic

equations. According to the analysis in [6], as long as the following equation is satisfied, the Richtmyer two-step difference Equation (17) is stable.

$$\begin{cases} \Delta t \le \dfrac{\Delta x}{|u| + c^*} \\ c^* = c = \sqrt{\dfrac{mp}{\rho}} \end{cases} \tag{18}$$

From Equation (18), when Δx is given, Δt must be less than the time taken by a sound wave to travel a distance Δx; that is a weak sound wave must not travel more than the space mesh width within a time interval. Thus:

$$\Delta t_j^n \le \frac{\Delta x}{\left|u_j^n\right| + \sqrt{\dfrac{mp_j^n}{\rho_j^n}}} \tag{19}$$

Generally, we took:

$$\Delta t^n = \min_j \left\{\Delta t_j^n\right\} \quad j = 0,1,2,\cdots,MM \tag{20}$$

as the next time interval in the numerical calculation.

During the actual calculation, the actual time interval is:

$$\Delta t_{cal}^n = CFL\Delta t^n \quad 0 < CFL \le 1 \tag{21}$$

where *CFL*, the stability coefficient, is in the range 0.90-0.95 if the method is stable. These stability conditions are known as the *CFL* conditions, after Courant, Friedrichs and Lewy, who wrote a paper in 1928 that used finite difference methods to prove the existence of solutions to the partial differential equations of mathematical physics.

5 Results and Discussion

Figure 2 shows the pressure-time histories at the three pressure gauge positions for the empty combustion simulator, showing that the maximum chamber pressure

attained in the early ignition process is approximately 2.7 MPa. The symbols p1, p2 and p3 in Figure 2 denote the pressure at the three gauge positions G1, G2 and G3, respectively. Since the ignition simulator is empty, there is no significant flow resistance at the three gauge positions. The flame spreading speed from G1 to G2 was approximate 100 mm·s^{-1}. However, due to heat loss to the air and the walls of the ignition simulator, the flame spreading speed from G2 to G3 had rapidly decreased to 70 mm·s^{-1}. The decrease of maximum pressure in the chamber is the result of heat loss along the wall. The pressure p1 at gauge G1 position responded earlier than the other gauges because G1 is located closer to the vent holes of the primer as seen in Figure 1.

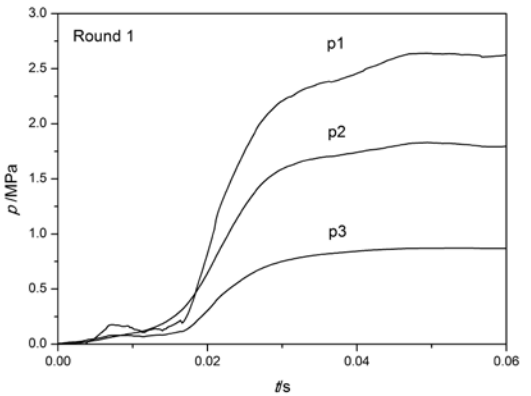

Figure 2. Pressure-time history at different positions in the empty ignition simulator (Round 1).

Figures 3 to 5 show the pressure-time histories and propagation in the 100 mm ignition simulator loaded with a granular pseudo-propellant bed at different porosities. Obviously, the igniter gases experienced significant flow resistance in the pseudo-propellant bed when the loading density was increased from 0.18 to 1.06 g·cm^{-3}. The flame spreading speed decreased from approximately 90 to 50 mm·s^{-1} between the G1 and G2 positions. Due to the heat loss to the ceramic pseudo-propellant bed, the maximum pressure decreased gradually with increased porosity. It should be noted that when the density of the pseudo-propellant bed was increased to 0.73 g·cm^{-3}, the pressure curves are fluctuated due to the axial movement of the pseudo-propellant along the ignition simulator, which was observed from the change of pseudo-propellant bed position when the ignition simulator was opened after the experiments. We also noted that there is a peak along the p1 curves after ignition when the density of the pseudo-propellant bed was increased to 0.73 and 1.06 g·cm^{-3}. The occurrence

of these peaks is believed to be associated with a change of gas flow through the pseudo-propellant bed, resulting from the change of permeability in local space. After the flow change, the pressure decreased gradually to the normal values.

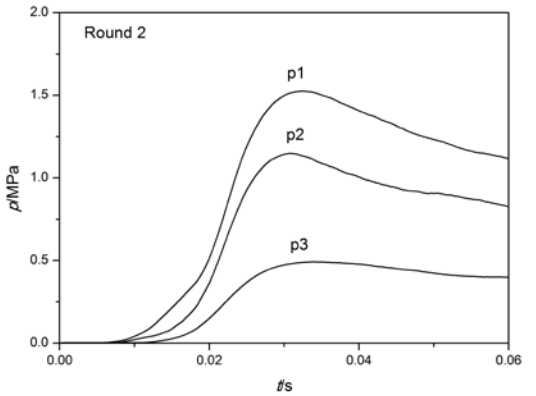

Figure 3. Pressure-time history at different positions in the ignition simulator when the loading density was 0.18 g·cm^{-3} (Round 2).

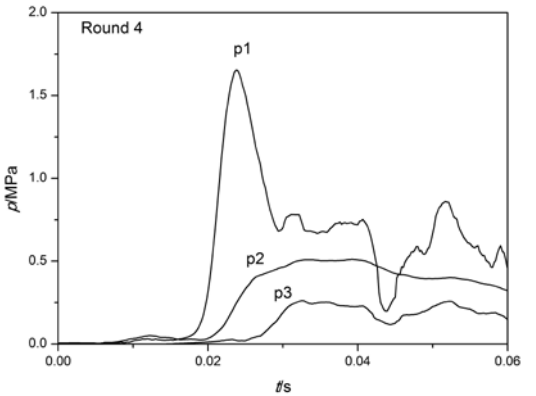

Figure 4. Pressure-time history at different positions in the ignition simulator when the loading density was 0.73 g·cm^{-3} (Round 4).

Figure 6 shows the numerical calculation results based on the rigid porous medium model described above. As seen in Figure 6, the calculated pressure values are verified by the experimental data at the low loading density of the pseudo-propellant bed of 0.18 g·cm^{-3}. However, when the loading density of the pseudo-propellant bed was increased to 0.73 and 1.06 g·cm^{-3}, shown in Figure 7, there is apparently a significant error between the experimental and the calculated results, especially in the early pressure peak at the G1 position closest to the

ignition primer. The most important reason for this deviation in the experimental result is the change of permeability of the pseudo-propellant bed in local space. When the ignition gas flows through the granular bed, the ignition pressure can result in the movement of the inert propellant bed in the simulator.

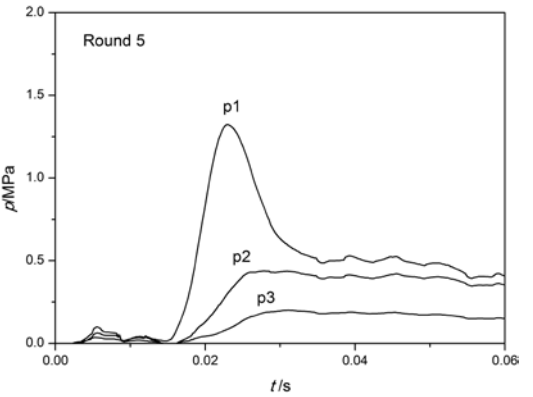

Figure 5. Pressure-time history at different positions in the ignition simulator when the loading density was 1.06 g·cm^{-3} (Round 5).

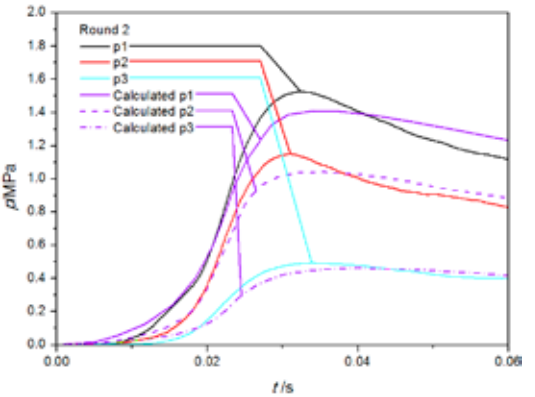

Figure 6. Experimental and calculated pressure-time histories at different positions in the ignition simulator when the loading density was 0.18 g·cm^{-3} (Round 2).

Due to the peak pressure rise and subsequent significant decrease resulting from the permeability of the pseudo-propellant bed, calculation is obviously more difficult under these circumstances. In spite of this, the established model of the ignition gas based on mechanical flow through a rigid porous medium could be used to describe and simulate the early pressure flow distribution in the pseudo-

propellant bed in the ignition simulator. The calculations can give some results that enable a better understanding of the physical processes of ignition gas flow in an ignition simulator loaded with a pseudo-propellant bed. Further simulation of the flame spreading process would need more sophisticated modelling and simulation, considering the movement of the pseudo-propellant bed and heat loss.

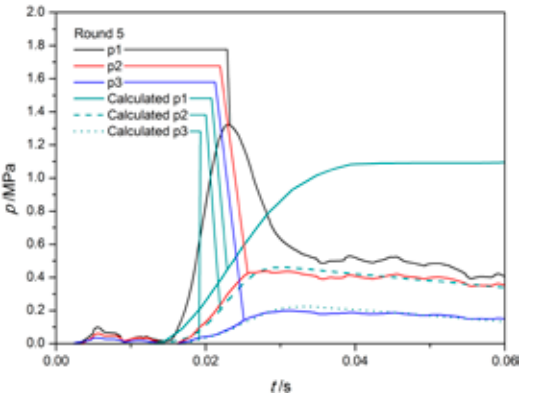

Figure 7. Experimental and calculated pressure-time histories at different positions in the ignition simulator when the loading density was 1.06 g·cm^{-3} (Round 5).

6 Conclusions

The theoretical model of ignition gas flow through a rigid porous medium is developed in order to calculate the pressure-time history at different positions along an ignition simulator loaded with a pseudo-propellant bed with different porosities. The established basic equations are hyperbolic in nature. The Richtmyer two-step method can be used to solve these equations. The initial results are based on the modelling of a pseudo-propellant bed considering only the purely "mechanical" flow process. Verification of the theoretical models were conducted by comparison of the calculated results with experimental data. The results showed that the theoretical model could describe and simulate the early pressure flow distribution in a pseudo-propellant bed in an ignition simulator. The calculations can enable a better understanding of the physical processes of the ignition gas flow. Further simulation of the flame spreading process would need more sophisticated modelling and simulation, considering the movement of the pseudo-propellant bed and heat loss.

Acknowledgement
This work was supported in part by the National Natural Science Foundation of China (No. 51376092).

7 References

[1] East Jr. J.I., Ignition and Flamespreading Phenomena in Granular Propellant Gun Charges, in: *Interior Ballistics of Guns*, (Krier H., Summerfield M., Eds.), American Institute of Aeronautics and Astronautics, **1979**, pp. 228-245.
[2] Chang L.-M., *Ignition Diagnostics of the 120-mm XM859-MP Cartridge*, Tech. Rep. BRL-TR-2840, U.S. Army Research Laboratory: Aberdeen Proving Ground, MD., **1987**.
[3] Kooker D.E., Chang L.-M., Howard S.L., *Flamespreading in Granular Solid Propellant: Design of an Experiment*, ARL-MR-80, U.S. Army Research Laboratory: Aberdeen Proving Ground, MD., **1993**.
[4] Kooker D.E., Howard S.L., Chang L.-M., *Flamespreading in Granular Solid Propellant: Initial Results*, ARL-TR-446, U.S. Army Research Laboratory: Aberdeen Proving Ground, MD., **1994**.
[5] Brant A.L., Colburn J.W., Ruth C.R., Worthington D.W., *Flamespreading Processes in Ball Powder Propellants*, ARL-TR-731, U.S. Army Research Laboratory: Aberdeen Proving Ground, MD., **1995**.
[6] Kooker D.E., Chang L.-M., Howard S.L., Convective Ignition of a Granular Solid Propellant Bed: Influence of Propellant Composition, *26th Symposium (Int.) on Combustion, Vol. II*, The Combustion Institute, Pittsburgh, Pennsylvania, USA, **1996**.
[7] Jaramaz S., Flamespreading during Base Ignition of Propellant Charge: Theoretical and Experimental Studies, *Propellants Explos. Pyrotech.*, **1997**, *22*(6), 326-332.
[8] Guo K.K., Ferrara P., *Flame Spreading and Combustion Behaviour of Gun Propellants Packed in High Loading Densities*, ADA426407, U.S. Army Research Laboratory: Aberdeen Proving Ground, MD., **2004**.
[9] May I.W., Horst A.W., Charge Design Considerations and Their Effect on Pressure Waves in Guns, in: *Interior Ballistics of Guns*, (Krier H., Summerfield M., Eds.), American Institute of Aeronautics and Astronautics, **1979**, pp. 197-227.
[10] Chang L.-M., Rocchio J.J., *Simulator Diagnostics of the Early Phase Ignition Phenomena in a 105-mm Tank Gun Chamber*, Tech. Rep. BRL-TR-2890, U.S. Army Ballistic Research Laboratory: Aberdeen Proving Ground, MD., **1988**.
[11] Miura H., Matsuo A., Nakamura Y., Three-Dimensional Simulation of Pressure Fluctuation in a Granular Solid Propellant Chamber within an Ignition Stage, *Propellants Explos. Pyrotech.,* **2011**, *36*(3), 259-267.
[12] Schmidt J.R., Nusca M.J., *Progress in the Development of a Multiphase Turbulent Model of the Gas/Particle Flow in a Small-caliber Ammunition Primer*, ARL-

TR-3860, U.S. Army Research Laboratory: Aberdeen Proving Ground, MD., **2006**.
[13] Nusca M.J., Howard S.L., *Experimental and Modelling Studies of Plasma Injection by an Electrothermal Igniter into a Solid Propellant Gun Charge*, ARL-TR-3806, U.S. Army Research Laboratory: Aberdeen Proving Ground, MD., **2006**.
[14] Song M., Porous Medium Models for the Early Stages in the Interior Ballistic Cycle, *ACTA Armamentarii*, **1992**, *31*(2), 12-18.
[15] Fu C., Zhang Z., Tan W., Numerical Simulation of Thermal Convection of a Viscoelastic Fluid in a Porous Square Box Heated from Below, *Phys. Fluids*, **2007**, *19*, 104-107.
[16] Xu F., Sofronics P., Aravas N., Meyer S., Constitutive Modelling of Porous Viscoelastic Materials, *Eur. J. Mech., A/Solids*, **2007**, *26*, 936-955.
[17] Allen M.B., Numerical Modelling of Multiphase Flow in Porous Media, *Adv. Water Resour.*, **1985**, *8*, 162-187.
[18] Collins R.E., *Flow of Fluids through Porous Material*, Reinhold Publishing Corporation, New York, **1961**.
[19] Fox P.J., Zhu Y., Morris J.P., *Fundamental Research on the Mechanicals of Fluid Flow through Porous Media*, Fin. Rep. ADA383619, Purdue University, West Lafayeett, IN, USA, **2000**.